Hindawi
Shock and Vibration
Volume 2021, Article ID 6669284, 16 pages
https://doi.org/10.1155/2021/6669284

Research Article

Investigation of Low-Frequency Sound Radiation Characteristics and Active Control Mechanism of a Finite Cylindrical Shell

Shaohu Ding, Chunyang Mu, Yang Gao, Hong Liu, and Maoqiang Li

College of Mechatronic Engineering, North MinZu University, Yinchuan, China

Correspondence should be addressed to Shaohu Ding; dingshaohu05@163.com

Received 15 December 2020; Revised 24 February 2021; Accepted 24 April 2021; Published 7 May 2021

Academic Editor: Chuanzeng Zhang

In this paper, the radiation characteristics and active structural acoustic control of a submerged cylindrical shell at low frequencies are investigated. First, the coupled vibro-acoustic equations for a submerged finite cylindrical shell are solved by a modal decomposition method, and the radiation impedance is obtained by the fast Fourier transform. The modal shapes of the first ten acoustic radiation modes and the structure-dependent radiation modes are presented. The relationships between the vibration modes and the radiation modes as well as the contributions of the radiation modes to the radiated sound power are given at low frequencies. Finally, active structural acoustic control of a submerged finite cylindrical shell is investigated by considering the fluid-structure coupled interactions. The physical mechanism of the active control is discussed based on the relationship between the vibration and radiation modes. The results showed that, at low frequencies, only the first several radiation modes contributed to the sound power radiated from a submerged finite cylindrical shell excited by a radial point force. By determining the radiation modes that dominate the contribution to the radiated sound, the physical mechanism of the active control is explained, providing a potential tool to allow active control of the vibro-acoustic responses of submerged structures more effectively.

1. Introduction

As a basic structural form, the cylindrical shell is commonly used in aerospace, marine, and other industrial fields. Such shell is excited to vibrate and radiate noise, and its vibro-acoustic characteristics have been widely concerned [1–5]. When a structure is immersed in a dense fluid (such as water), the vibration of the structure produces sound waves, causing the surrounding medium to vibrate, and in turn, the sound pressure acting on the structure as the excitation complicates the analysis of structural vibration. The sound behavior of a shell in water is very different from that in air, and as such, has received considerable attention [3–5]. To analyze the structural vibrations and sound radiation of fluid-loaded structures, many researchers investigated the effect of both external and internal fluid on shell vibrations taking into account the fluid-structure interaction. Junger [6] and Sandman [7] expanded the radial displacement of the cylindrical surface into Fourier series along the circumference. They expressed the radiated sound pressure in terms of acoustic impedance through the boundary conditions of the fluid-solid interface. Amabili [8–10] studied the coupled vibration of shell-external fluid and shell-internal fluid and presented the solution for cylindrical shells filled and partially immersed in incompressible and compressible fluid. Kwak [11] investigated free flexural vibration of a finite cylindrical shell in contact with external fluid. The kinetic energy of the fluid is derived by solving the boundary-value problem. At the same time, many researchers have sought to develop efficient methods to reduce the noise of cylindrical structures. Generally, these methods can be divided into two subgroups. The first group contains passive methods, which reduce the noise of a structure using additional mass, dynamic vibration absorber, or viscoelastic damping material on the structure surface. The second subgroup contains active methods [12–17], which reduce the structurally radiated noise using actuators, sensors, and control algorithms. The passive method is not satisfactory in noise reduction in the low-frequency range. Therefore, the active control method, as an alternative to the passive

control method, has been used in noise control in the low-frequency range.

There have been a lot of literatures on the vibro-acoustic characteristics of cylindrical shells. However, to use active structural sound control methods to effectively suppress the radiated noise of cylindrical shells, it is necessary to understand the modal characteristics of the vibration and radiation of the cylindrical shell in the low-frequency range. Sepanishen [2] investigated the radiation impedance of an infinite cylinder with a finite-length, nonuniform velocity distribution. Chen et al. [18] explored the modal radiation efficiency and radiation power of stiffened double-cylindrical shells considering the fluid field between the inner shell and outer shell. The results show that radiation efficiency and radiation power were affected mainly by the low-order modes at low frequencies. Lin et al. [19] discussed the modal characteristics of sound radiation of finite cylindrical shells using boundary element methods. The results show that, for each group of modes with the same circumferential modal index, the modal radiation efficiency decreases as the axial modal index increases. Peters et al. [20] presented a modal decomposition technique to analyze individual modal contributions to the sound power radiated from an externally excited structure submerged in a dense fluid. To control the structural vibrations and sound radiation of fluid-loaded structures, there have been few reports focused on vibration control through modal approaches and even fewer reports dealing with the modal control of vibrations and sound radiation [21, 22].

A thorough exploration of the vibrations and sound radiation would be conducive to understand the physical mechanism of the active noise reduction, provide guidance for optimal design, determine the arrangement of the actuators and the sensors, and select the control target. Structural vibration modes can be used to investigate the mechanism of structural acoustic radiation [23]. However, the sound radiation of each structural vibration mode is not independent, as the modes are coupled [24]. This creates difficulties when analyzing the structural acoustic radiation using structural vibration modes. In the early 1990s, Elliott and Johnson [23] presented the theory of acoustic radiation modes (a-modes) and decomposed the total sound power radiated from an elastic structure into a superposition of finite radiation modes. Each radiation mode was independent. These modes were only determined by the shape and size of the vibrating structure, and they were unrelated to the physical properties and boundary conditions of the structure. The advantages of acoustic radiation modes have attracted significant attention for the analysis and control of structural acoustic radiation in recent years [25–29]. In our previous research [30], we discussed the contribution of the low-order vibration modes and acoustic radiation modes to the radial squared velocity and the radiated sound power in different fluids and found that compared in water, more vibration modes and acoustic radiation modes are required to calculate the sound power in air. To accurately predict the vibro-acoustic behavior of a structure, the concept of structure-dependent radiation modes (s-modes) was presented by Photiadis [31] and developed by Ji and Bolton [32] to describe the sound power radiation from a simple vibrating beam and a thin baffled plate. Compared with a-modes, s-modes have more potential advantages because the sound power radiation is related to the boundary conditions and the material properties of the structure. However, previous studies on acoustic radiation modes and structure-dependent radiation modes are mostly for flat structures, and considerable research has been conducted on the vibration modes of cylindrical shells. There has been little research on acoustic radiation modes and structure-dependent radiation modes of the cylindrical shell. Further, several articles have examined the active structural acoustic control of submerged finite cylindrical shells [33–36]. However, few literatures explored the physical mechanism analysis of active control by using the relationship between the vibration modes and radiation modes.

In this work, by means of a modal expansion approach, the coupled vibro-acoustic equations for a finite cylindrical shell are solved first. The radiation impedance, which expresses the modal coupling caused by the fluids, is then obtained using the fast Fourier transform. Second, the modal shapes of the first few acoustic radiation modes and structure-dependent radiation modes are presented. The contributions of the low-order radiation modes to the sound power are discussed for a cylindrical shell immersed in a dense fluid using the solution of the vibration equation. The active structural acoustic control of a submerged finite cylindrical shell is investigated by considering the fluid-structure coupling interaction. An analytical expression for the optimal complex amplitude of the secondary force is derived based on the uncoupled characteristics of the sound power radiated from the finite cylindrical shell in the circumferential direction. The control effects with one and two control forces are also compared. Finally, the physical mechanism of the active structural acoustic control of the submerged finite cylindrical shell is analyzed based on the changes of the amplitude and sound power of the acoustic radiation modes and the structure-dependent radiation modes.

2. Theory

2.1. Theoretical Modeling Approach. A finite cylindrical shell with two semi-infinite cylindrical rigid baffles is considered, as illustrated in Figure 1; L is the length of the shell and h and a denote the wall thickness and radius of the shell, respectively. The shell is immersed in an unbounded fluid whose density is ρ_l, and the speed of sound in this fluid is c_l. The fluid is assumed to be stationary, nonviscous, and compressible.

In this study, the Flügge equations of motion are used to model the fluid-loaded cylindrical shell. The fluid-structure interaction problem is solved using an infinite shell model, which is shown to be a good approximation for finite shells [5]. The mathematical problem to be solved according to Flügge shell theory is

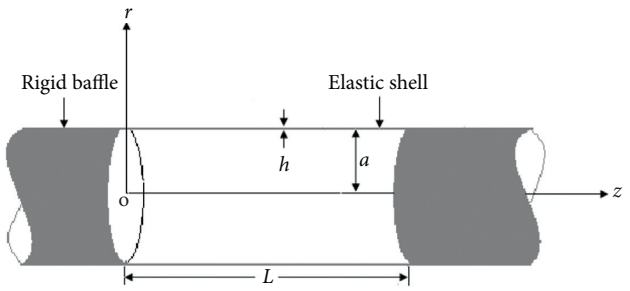

Figure 1: Baffled cylindrical shell and coordinate system.

$$\{\mathbf{L}_{3\times3}\}\begin{bmatrix} u(r,\phi,z) \\ v(r,\phi,z) \\ w(r,\phi,z) \end{bmatrix} = \frac{\left(1-\nu^2\right)a^2}{E^* h}\left(\begin{bmatrix} f_u \\ f_v \\ f_w - p_w \end{bmatrix}\right), \tag{1}$$

where $\mathbf{L}_{3\times3}$ refers to the coefficient matrix of the Flügge operator, the elements of which is given in Appendix A, and u, v, and w are the displacements of cylindrical shells in the x-, ϕ-, and z-directions, respectively. $E^* = E(1-i\eta)$ is the complex Young's modulus; η is the damping loss factor; f_u, f_v, and f_w are the excitation forces of the cylindrical shell in the x-, ϕ-, and z-directions, respectively; and, p_w represents the fluid load on the shell surface.

When simply supported boundary conditions are considered and the time-dependent factor of $e^{-i\omega t}$ is omitted, the displacement of the cylindrical shells in the x-, ϕ-, and z-directions can be expressed as

$$\begin{aligned} u(z,\phi) &= \sum_{\alpha=0}^{1}\sum_{n=0}^{\infty}\sum_{m=1}^{\infty} C_{umn}^{\alpha}\cos(k_m z)\sin\left(n\phi+\frac{\alpha\pi}{2}\right) \\ &= \sum_{n=0}^{\infty} u_n(z,\phi), \\ v(z,\phi) &= \sum_{\alpha=0}^{1}\sum_{n=0}^{\infty}\sum_{m=1}^{\infty} C_{vnm}^{\alpha}\sin(k_m z)\cos\left(n\phi+\frac{\alpha\pi}{2}\right) \\ &= \sum_{n=0}^{\infty} v_n(z,\phi), \\ w(z,\phi) &= \sum_{\alpha=0}^{1}\sum_{n=0}^{\infty}\sum_{m=1}^{\infty} C_{wnm}^{\alpha}\sin(k_m z)\sin\left(n\phi+\frac{\alpha\pi}{2}\right) \\ &= \sum_{n=0}^{\infty} w_n(z,\phi), \end{aligned} \tag{2}$$

where subscripts n ($n = 0, 1, 2, \ldots$) and m ($m = 1, 2, 3, \ldots$) correspond to the circumferential mode index and axial mode index, respectively, $k_m = m\pi/L$ is the axial wavenumber, C_{jmn}^{α} is the modal displacement response amplitude of the shell in the x-, θ-, and z-directions, $\alpha = 0$ corresponds to antisymmetric modes, and $\alpha = 1$ corresponds to symmetric modes. In this study, the disturbance force and control force are assumed to be located at $\phi = 0$ or π. Therefore, only the symmetric modes are excited by such a force configuration for vibration analysis and noise control, which indicates that the displacements for each circumferential mode can be written as

$$\begin{aligned} u_n(z,\phi) &= \sum_{m=1}^{\infty} C_{unm}^{1}\cos(k_m z)\cos(n\phi), \\ v_n(z,\phi) &= \sum_{m=1}^{\infty} C_{vnm}^{1}\sin(k_m z)\sin(n\phi), \\ w_n(z,\phi) &= \sum_{m=1}^{\infty} C_{wnm}^{1}\sin(k_m z)\cos(n\phi). \end{aligned} \tag{3}$$

Considering fluid-structure coupling, the motion equation of the cylindrical shell is as follows [1]:

$$M_{mn}\left[\omega_{mn}^2(1-i\eta)-\omega^2\right]C_{wnm}^{1} = F_{mn} - P_{mn}, \tag{4}$$

where M_{mn} denotes the generalized modal mass of the shell, ω_{mn} represents the in-vacuo natural angular frequencies, η is the structural damping coefficient, and F_{mn} is the generalized modal excitation force, which can be described as follows:

$$\begin{aligned} F_{mn} &= \frac{\varepsilon_n}{\pi L}\int_0^{2\pi}\int_0^{L} f(z_0,\phi_0)\sin\left(\frac{m\pi z}{L}\right)\cos(n\phi)\,dz\,d\phi \\ &= f_0\varphi_{mn}, \end{aligned} \tag{5}$$

where ε_n is the Neumann factor ($\varepsilon_n = 1$ for $n = 0$ and $\varepsilon_n = 2$ for $n > 0$), $f(z_0,\phi_0) = (f_0/a)\delta(z_0)\delta(\phi_0)$ is the harmonic point force applied in the radial direction of the cylindrical shell, $\varphi_{mn} = (\varepsilon_n/2\pi La)\cos(n\phi_0)sin(k_m z_0)$, and f_0 is the complex amplitude of the excitation force.

The modal sound pressure induced by the fluid is denoted as P_{mn}, the expression of which is derived in detail in the Appendix B, and can be expressed as follows:

$$P_{mn} = -i\omega a\sum_{q=1}^{\infty} C_{wnm}^{1} Z_{qmn}, \tag{6}$$

where Z_{qmn} is the radiation impedance, which expresses the modal coupling between the different axial modal indices (m and q) due to the fluids. It can be obtained by the fast Fourier transform, which can significantly reduce the analysis time compared with traditional direct numerical integration methods [37]:

$$Z_{qmn} = \frac{2}{L}\int_0^{L}\mathscr{F}^{-1}\left[\tilde{z}_n(k_z)\mathscr{F}\left[f_q(z)\right]\right]\sin k_m z\,dz, \tag{7}$$

where

$$\begin{aligned} \tilde{z}_n(k_z) &= \frac{i\omega\rho_l H_n\left[\left(k^2-k_z^2\right)^{1/2}a\right]}{\left(k^2-k_z^2\right)^{1/2}H_n'\left[\left(k^2-k_z^2\right)^{1/2}a\right]}, \\ f_q(z) &= \begin{cases} \sin k_q z, & 0\le z\le L \\ 0, & z<0, z>L \end{cases}, \\ \mathscr{F}\left[f_q(z_q)\right] &= \frac{k_q\left[1-(-1)^q e^{-ik_z L}\right]}{k_q^2-k_z^2}, \end{aligned} \tag{8}$$

where $\mathscr{F}$ and $\mathscr{F}^{-1}$ represent the Fourier transform and inverse Fourier transform, respectively, $k = \omega/c_l$ is the fluid wavenumber, $k_q = q\pi/L$, k_z is the structural axial wavenumber, H_n is the nth-order Hankel function of the second kind for a radially outgoing wave, and H_n' is the derivative of the Hankel function with respect to its argument.

Substituting equations (5) and (6) into equation (4), the radial displacement amplitude of the shell C_{wnm}^1 can be obtained. Then, the radiated sound power of the fluid-loaded cylinder will be acquired.

2.2. Acoustic Radiation Modes of Finite Cylindrical Shells. Using the transfer acoustic impedance matrix $\mathbf{Z}$, the modal contributions to the radiated sound power can be acquired. It is well-known acoustic radiation modes that correspond to the eigenvectors of the resistive part of the sound impedance matrix. The acoustic radiation modes are a set of orthonormal surface velocity patterns. At low frequencies, only the first few sound radiation modes are radiated efficiently. Therefore, the total radiated sound power can be obtained by truncating the series sound radiation modes without loss of calculation accuracy.

The surface of the cylindrical shell is evenly split into N_e elementary radiators, where the area of each elementary radiator is denoted as s. The radiated sound power can be obtained through the near-field method, as follows [18]:

$$W = \frac{s}{2}\mathrm{Re}\left(\mathbf{V}^{\mathrm{H}}\mathbf{Z}\mathbf{V}\right) = \mathbf{V}^{\mathrm{H}}\mathbf{R}\mathbf{V}, \tag{9}$$

where $\mathbf{V}$ is the complex velocities' vector of these elementary radiators, the superscript "H" denotes the conjugate transpose, and $\mathbf{R} = (s/2)\mathrm{Re}(\mathbf{Z})$ is a real, symmetric, positive definite matrix, which is proportional to the transfer acoustic impedance matrix for the elementary radiators. These matrix elements can be expressed as follows [38]:

$$R_{ij} = \frac{s}{2}\mathrm{Re}\left\{\frac{i\omega\rho_l s}{2\pi^2}\sum_{n=0}^{\infty}\varepsilon_n\cos\left[\left(\theta_i-\theta_j\right)\right]\int_0^{k_0}\frac{\cos k_z\left(z-z'\right)}{\sqrt{k^2-k_z^2}\,a}\frac{H_n\left[\left(k^2-k_z^2\right)^{1/2}a\right]}{H_n'\left[\left(k^2-k_z^2\right)^{1/2}a\right]}dk_z\right\}, \tag{10}$$

where $\mathbf{R}$ can be expressed through an eigenvector decomposition as follows:

$$\mathbf{R} = \mathbf{Q}^{\mathrm{T}}\mathbf{\Lambda}\mathbf{Q}, \tag{11}$$

where $\mathbf{Q}$ is an orthogonal matrix of eigenvectors and Λ is a diagonal matrix of eigenvalues. Substituting equation (11) into equation (9) and defining $y = \mathbf{Q}\mathrm{V}$, equation (9) can be written as follows:

$$W = y^H\Lambda y = \sum_{k=1}^{K}\lambda_k\left|y_k\right|^2, \tag{12}$$

where $y_k = q_k^{\mathrm{T}}\mathbf{V}$ denotes the modal amplitude of the kth radiation mode, q_k is the kth radiation modal shape vector, and λ_k is called the radiation efficiency coefficient of the kth acoustic radiation mode. As shown by equation (8), the radiation modes radiate independently, and the sound power becomes a summation of independent quantities y_k factored by the eigenvalue λ_k.

2.3. Structure-Dependent Radiation Modes. If the vibration response of the structure is represented by the superposition of the modal vibration response, the surface velocity of the structure can be expressed by the vibration modes as follows:

$$\mathbf{V} = \mathbf{\Phi}\widehat{V}_N, \tag{13}$$

where $\widehat{V}_N$ is the corresponding modal coefficient vector, which is an $N \times 1$ column vector, N is the number of vibration modes, and $N = m \times n$:

$$\widehat{V}_N = \left[\,\widehat{V}_{m1}\;\;\widehat{V}_{m2}\;\;\ldots\;\;\widehat{V}_{mn}\,\right]^{\mathrm{T}}. \tag{14}$$

Φ is an $N_e \times N$ structural mode shape matrix defined as follows:

$$\boldsymbol{\Phi} = \begin{bmatrix} \sin\frac{\pi z_1}{L}\cos\varphi_1 & \sin\frac{\pi z_1}{L}\cos 2\varphi_1 & \cdots & \sin\frac{2\pi z_1}{L}\cos\varphi_1 & \sin\frac{2\pi z_1}{L}\cos 2\varphi_1 & \cdots & \sin\frac{m\pi z_1}{L}\cos n\varphi_1 \\ \sin\frac{\pi z_1}{L}\cos\varphi_2 & \sin\frac{\pi z_1}{L}\cos 2\varphi_2 & \cdots & \sin\frac{2\pi z_1}{L}\cos\varphi_2 & \sin\frac{2\pi z_1}{L}\cos 2\varphi_2 & \cdots & \sin\frac{m\pi z_1}{L}\cos n\varphi_2 \\ \cdots & \cdots & \cdots & \cdots & \cdots & \cdots & \cdots \\ \sin\frac{\pi z_2}{L}\cos\varphi_1 & \sin\frac{\pi z_2}{L}\cos 2\varphi_1 & \cdots & \sin\frac{2\pi z_2}{L}\cos\varphi_1 & \sin\frac{2\pi z_2}{L}\cos 2\varphi_1 & \cdots & \sin\frac{m\pi z_2}{L}\cos n\varphi_2 \\ \sin\frac{\pi z_2}{L}\cos\varphi_2 & \sin\frac{\pi z_2}{L}\cos 2\varphi_2 & \cdots & \sin\frac{2\pi z_2}{L}\cos\varphi_2 & \sin\frac{2\pi z_2}{L}\cos 2\varphi_2 & \cdots & \sin\frac{m\pi z_2}{L}\cos n\varphi_2 \\ \cdots & \cdots & \cdots & \cdots & \cdots & \cdots & \cdots \\ \sin\frac{\pi z_{Nz}}{L}\cos\varphi_{N\varphi} & \sin\frac{\pi z_{Nz}}{L}\cos 2\varphi_{N\varphi} & \cdots & \sin\frac{2\pi z_{Nz}}{L}\cos\varphi_{N\varphi} & \sin\frac{2\pi z_{Nz}}{L}\cos 2\varphi_{N\varphi} & \cdots & \sin\frac{m\pi z_{Nz}}{L}\cos n\varphi_{N\varphi} \end{bmatrix}. \quad (15)$$

Substituting equation (13) into equation (9), the radiated sound power can be further expressed as

$$W = \mathbf{V}^{\mathrm{H}}\mathbf{R}\mathbf{V} = \widehat{V}_N{}^{\mathrm{H}}\mathbf{G}\widehat{V}_N \quad (16)$$

where $\mathbf{G} = \Phi^{\mathrm{H}}\mathbf{R}\Phi$, which is also a real symmetric positive definite matrix. Each element is considered to be the contribution of the ith mode to the structural acoustic radiation due to the vibration of the jth mode. The case where $i = j$ represents the contribution of the mode vibrations of the structure itself to the radiated sound power, and the contribution of such self-radiation to the total sound power is always dominant near the natural frequency. Its off-diagonal elements represent the contribution of the modes to the radiated sound power caused by other modes, and the values are often much smaller than the diagonal elements of the matrix.

The dimension of $\mathbf{G}$ is not only related to the number of partition elements on the structure surface but also to the number of vibration modes. It can be decomposed into the following eigenvalues:

$$\mathbf{G} = \mathrm{P}^{\mathrm{H}}\boldsymbol{\Sigma}\mathrm{P}, \quad (17)$$

where $\mathbf{P}$ is an orthogonal matrix, the eigenvectors corresponding to each row of the matrix, Σ is a diagonal matrix composed of the N eigenvalues, which are different from those defined in equation (12), and $\sigma_r$is called the radiation efficiency coefficient of the rth structure-dependent radiation mode. The matrix $\mathbf{G}$ is a real symmetric positive definite matrix, and thus, the eigenvalues have the following characteristics $\sigma_1 > \sigma_2 > \sigma_3, \cdots, > \sigma_r > 0$.

Substituting equation (17) into equation (16), the radiated sound power can be further expressed as

$$W = \widehat{V}_N^{\mathrm{H}}\mathrm{P}^{\mathrm{H}}\boldsymbol{\Sigma}\mathrm{P}\widehat{V}_N. \quad (18)$$

Defining

$$\mathbf{g} = \mathrm{P}\widehat{V}_N. \quad (19)$$

The radiated sound power can be further expressed as

$$W = \mathbf{g}^{\mathrm{H}}\boldsymbol{\Sigma}\mathbf{g} = \sum_{r=1}^{N}\sigma_r\left|g_r\right|^2, \quad (20)$$

where N represents the number of vibration modes and g_r is the vector of linear transformations of the modal velocity amplitude of the structure surface through the transformation matrix, which is defined as the structural radiation mode vector.

2.4. Active Control of Sound Radiation from the Submerged Cylindrical Shell. Assuming that the primary force (i.e., disturbance input) is a harmonic radial point force with a known amplitude, the secondary forces (control inputs) are also one or more harmonic point forces. The objective function of the active control is the sound power radiated from the cylindrical shells subjected to primary and secondary forces. The expression of the complex amplitude of the secondary control forces is derived when minimizing the objective function.

Due to the fluid-structure interaction, the modal velocity and radiated sound power cannot be directly represented in a matrix form such that the complex amplitude of the secondary control forces can be solved easily. Because the radiated sound power of the different circumferential vibration modes is decoupled from each other [25], the radiated sound power can be determined individually for each circumferential vibration mode:

$$W = \sum_{n=0}^{\infty} W_n. \tag{21}$$

The sound power of the nth-order circumferential vibration mode can be expressed in the matrix form:

$$W_n = \widehat{V}_n{}^{\mathbf{H}} \mathbf{M}_n \widehat{V}_n, \tag{22}$$

where $\boldsymbol{M}_n$ represents the $M \times P$ radiation resistance matrix corresponding to the nth-order circumferential mode.

For a selected circumferential mode, equation (4) can be written as follows:

$$\begin{pmatrix} Z_{1n}^M + Z_{11n} & Z_{12n} & \cdots & Z_{1pn} \\ Z_{21n} & Z_{2n}^M + Z_{22n} & \cdots & Z_{2pn} \\ \cdots & \cdots & \cdots & \cdots \\ Z_{1mn} & Z_{2mn} & \cdots & Z_{mn}^M + Z_{qmn} \end{pmatrix} \begin{pmatrix} \widehat{V}_{1n} \\ \widehat{V}_{2n} \\ \cdots \\ \widehat{V}_{mn} \end{pmatrix} = \begin{pmatrix} f_{1n} \\ f_{2n} \\ \cdots \\ f_{mn} \end{pmatrix}, \tag{23}$$

where Z_{mn}^M denotes the modal mechanical impedance of the shell. $\widehat{V}_{mn} = -i\omega C_{wmn}^1$ is the modal vibration velocities of cylindrical shells in the z-directions.

Therefore, the modal vibration velocities corresponding to the nth-order circumferential mode can be expressed as

$$\mathbf{V}_n = [\mathbf{Z}_n]^{-1} \cdot [\mathbf{F}_n], \tag{24}$$

where $\boldsymbol{F}_n$ is an $M \times 1$ column vector that represents the modal excitation force corresponding to the nth-order circumferential mode, which includes two parts: a primary modal excitation force $\mathbf{F}_n^P$ that consists of a $Q \times 1$ column vector and a secondary modal excitation force $\mathbf{F}_n^S$ that consists of a $K \times 1$ column vector:

$$\begin{aligned} \mathbf{F}_n^P &= \boldsymbol{\psi}_n^P \mathbf{f}_p = \begin{pmatrix} \varphi_{11}^P & \varphi_{12}^P & \cdots & \varphi_{1Q}^P \\ \varphi_{21}^P & \varphi_{22}^P & \cdots & \varphi_{2Q}^P \\ \cdots & \cdots & \cdots & \cdots \\ \varphi_{m1}^P & \varphi_{m2}^P & \cdots & \varphi_{mQ}^P \end{pmatrix} \begin{pmatrix} f_{p1} \\ f_{p2} \\ \cdots \\ f_{pQ} \end{pmatrix}, \\ \mathbf{F}_n^S &= \boldsymbol{\psi}_n^S \mathbf{f}_s = \begin{pmatrix} \varphi_{11}^S & \varphi_{12}^S & \cdots & \varphi_{1K}^S \\ \varphi_{21}^S & \varphi_{22}^S & \cdots & \varphi_{1K}^S \\ \cdots & \cdots & \cdots & \cdots \\ \varphi_{m1}^S & \varphi_{m2}^S & \cdots & \varphi_{mK}^S \end{pmatrix} \begin{pmatrix} f_{s1} \\ f_{s2} \\ \cdots \\ f_{sK} \end{pmatrix}, \end{aligned} \tag{25}$$

where $\mathbf{f}_p$ represents the complex amplitude vector of the primary modal excitation force, $\mathbf{f_s}$ represents the complex amplitude vector of the secondary modal excitation force, and ψ_n^P and ψ_n^S represent primary and secondary modal force coordinate vectors corresponding to the nth-order circumferential mode, and their elements can be obtained using equation (5).

Consequently, equation (24) becomes

$$\widehat{V}_n = \widehat{V}_n^P + \widehat{V}_n^S = \mathbf{T}_p \mathbf{f}_p + \mathbf{T}_s \mathbf{f}_s, \tag{26}$$

where $\mathbf{T}_p = [\mathbf{Z}_n]^{-1} \psi_n^P$ and $\mathbf{T}_s = [\mathbf{Z}_n]^{-1} \psi_n^S$ represent the transfer functions between the structural response and the primary and secondary excitation forces, respectively.

Substituting equation (26) into equation (22), we obtain

$$\begin{aligned} W &= \sum_{n=0}^{\infty} \widehat{V}_n{}^{\mathbf{H}} \mathbf{M}_n \widehat{V}_n = \sum_{n=0}^{\infty} \left[\left(\mathbf{T}_p \mathbf{f}_p + \mathbf{T}_s \mathbf{f}_s \right)^{\mathbf{H}} \mathbf{M}_n \left(\mathbf{T}_p \mathbf{f}_p + \mathbf{T}_s \mathbf{f}_s \right) \right] \\ &= \mathbf{f}_p{}^{\mathbf{H}} \sum_{n=0}^{\infty} \left(\mathbf{T}_p{}^{\mathbf{H}} \mathbf{M}_n \mathbf{T}_p \right) \mathbf{f}_p + \mathbf{f}_p{}^{\mathbf{H}} \sum_{n=0}^{\infty} \left(\mathbf{T}_p{}^{\mathbf{H}} \mathbf{M}_n \mathbf{T}_s \right) \mathbf{f}_s \\ &\quad + \mathbf{f}_s{}^{\mathbf{H}} \sum_{n=0}^{\infty} \left(\mathbf{T}_s{}^{\mathbf{H}} \mathbf{M}_n \mathbf{T}_p \right) \mathbf{f}_p + \mathbf{f}_s{}^{\mathbf{H}} \sum_{n=0}^{\infty} \left(\mathbf{T}_s{}^{\mathbf{H}} \mathbf{M}_n \mathbf{T}_s \right) \mathbf{f}_s. \end{aligned} \tag{27}$$

The radiation sound power can be expressed as a quadratic function of the complex amplitude of the control input, i.e., the Hermitian quadratic form. Consequently, the optimal strength of the secondary source for active control can be obtained for the active control as follows:

$$\mathbf{f}_s = -\left[\sum_{n=0}^{\infty} \left(\mathbf{T}_s{}^{\mathbf{H}} \mathbf{M}_n \mathbf{T}_s \right) \right]^{-1} \sum_{n=0}^{\infty} \left(\mathbf{T}_s{}^{\mathbf{H}} \mathbf{M}_n \mathbf{T}_p \right) \mathbf{f}_p. \tag{28}$$

The calculated optimal secondary force can be inserted into equation (27), and the radiated sound power with active control can be obtained.

3. Results and Discussion

A finite cylindrical shell submerged in fluid is schematically shown in Figure 1. The structure is made of steel (density $\rho_s = 7850\,\text{kg/m}^3$, Young's modulus $E = 2.1 \times 10^{10}\,\text{N/m}^2$, and Poisson's ratio $\sigma = 0.3$). The density and speed of sound of the fluid are $\rho_l = 1000\,\text{kg/m}^2$ and $c_l = 1500\,\text{m/s}$, respectively, for water. The structural damping is introduced by means of a complex elastic modulus, i.e., $E(1 - i\eta)$, where $\eta = 0.01$ is the damping loss factor of the shell. It is assumed that the radial excitation force is centered at a point $z_0 = 0.44$ and $\phi_0 = 0$. Its magnitude is 1 N and along the radial direction of the shell.

In order to evaluate the accuracy of the proposed model, the natural frequencies of a cylindrical shell in air and in water obtained here are compared with those from the literature and are listed in Table 1. Good agreement between values obtained from the present model with results from the literature can be observed.

3.1. Radiation Modal Characteristics. For a finite cylindrical shell with $L = 1.2\,\text{m}$, $a = 0.4\,\text{m}$, and $h = 0.003\,\text{m}$, the surface is divided into 20×36 equal area units for the numerical calculations. Each radiation mode q_k has a different shape. Figure 2 shows the modal shapes of the first ten acoustic radiation modes for $kL = 1$.

As shown in Figure 2, the acoustic radiation modes of the submerged finite cylindrical shells are composed of

Table 1: Comparison of values of the natural frequency (Hz) for a shell $L = 1.284$ m, $a = 0.18$ m, and $h = 0.003$ m.

m	n	Air			Water		
		Ref. [39]	Ref. [40] *	Present	Ref. [39]	Ref. [40] *	Present
1	5	542.3	—	542.8	351.6	—	343
1	4	340.5	336.6	340.5	205.6	200.9	202
1	2	195.3	194.0	197.1	98.2	97.5	99
1	3	199.0	198.0	198.8	110.9	108.7	109
2	2	635.8	—	654.7	328.9	—	339
2	3	386.5	387.0	388.5	218.2	217.0	217
2	4	403.5	403.0	403.4	245.8	241.3	242
2	5	570.0	—	570.2	380.8	—	362
3	4	568.1	—	567.7	350.2	—	344

* Experimental results.

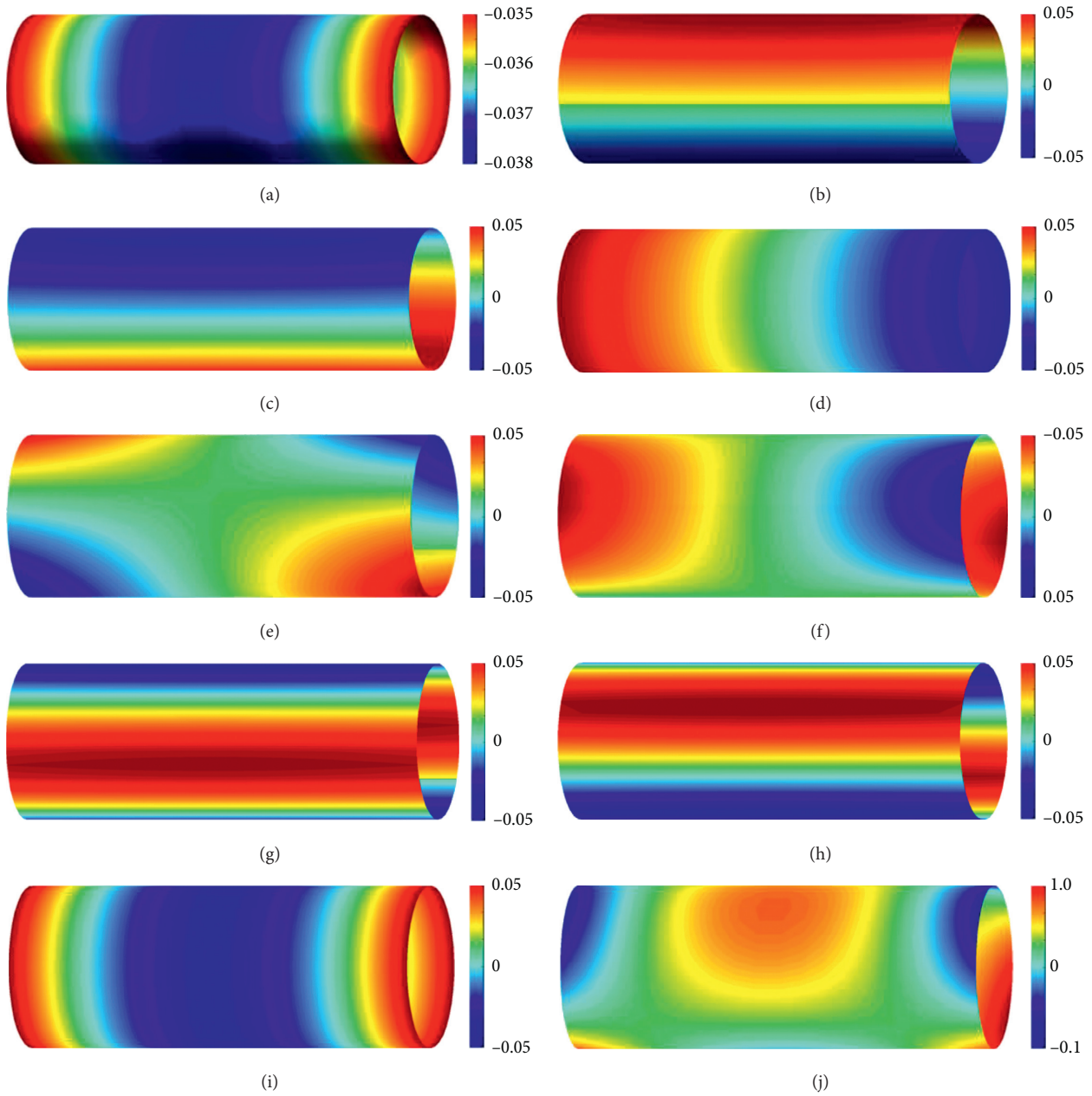

Figure 2: Modal shapes of the first ten a-modes ($kL = 1$) (a–j) for the modes from first to tenth.

symmetric and antisymmetric vibration modes. The velocity distribution corresponding to the first radiation mode is uniform in the middle of the shell, and the radiation type is similar to a monopole source. The velocity patterns corresponding to the second and third radiation modes are distributed uniformly along the axial direction and are symmetric and antisymmetric in the circumferential direction. Thus, these can be called circumferential dipole modes. The fourth radiation mode is an axial dipole mode, and the radiation modes from fifth to eighth are analogous with quadrupole modes. The fifth and six modes are compound axial and circumferential quadrupole modes, and the seventh and eighth radiation modes are circumferential quadrupole modes.

From equation (16), it is seen that if the surface velocity vector is expressed in terms of the vibration modes of the structure, the structure-dependent radiation mode shapes can reflect the relationship between radiation modes and vibration modes. The first ten axial and circumferential structural vibration modes occur within the frequency range of interest. In Figure 3, discrete integer values up to 100 on the horizontal axis represent cylindrical shell vibration modes (m, n) corresponding to (1,0), (1,1), (1,2) ... (1,9), (2,0),(2,1), (2,2), ..., (10,9). The first six s-modes' shapes are rendered against the structural vibration modes in Figure 3.

Compared with the s-mode shapes of beams and plates [32], the s-mode shapes of a finite cylindrical shell with simply supported boundary conditions are more complicated, as shown in Figure 3. All the s-mode shapes possess many modal nodes, and each node corresponds to a structure vibration mode, i.e., if the sound power generated by a single s-mode is calculated, the vibration modes at the nodes do not contribute to the sound power generated by this s-mode, regardless of the velocity magnitude of these vibration modes, and only the vibration modes with nonzero values will contribute. At low frequencies, each s-mode is associated with a few vibration modes. It can be seen from Figure 3(a) that the first s-mode shapes possess peaks at modes 1, 21, 41, 61, and 81, corresponding to the structural vibration modes (1, 0), (3, 0), (5, 0), (7, 0), and (9, 0) of the cylindrical shell. Thus, the sound power radiated from these vibration modes could be replaced by the sound power generated from the first s-mode. With the increase in the number of the axial vibration mode, the amplitude of the structure-dependent radiation modes decreases gradually, which indicates the contribution of the vibration modes to the amplitude of the structure-dependent radiation mode decrease. At the same time, the 4th s-mode corresponds to the same structural modes as well as the first s-mode; however, these two s-modes correspond to different dominant structural vibration modes. The dominant mode of the first s-mode corresponds to vibration mode (1, 0), while the dominant mode of the 4th s-mode corresponds to vibration mode (3, 0). It also can be seen from Figure 2 that the 1st and 4th a-modes in the circumferential direction are not pitch line and have similar circumferential vibration patterns, similar to the vibration modes with $n = 0$. In addition, the structural modes for (1, 0), (3, 0), (5, 0), (7, 0), and (9, 0) tend to form dipole radiation. The 2nd s-modes mainly have peaks at the 2, 22, 42, 62, and 82 vibration modes, which correspond to the vibration modes (1,1), (3,1), (5,1), (7,1), and (9,1) of the cylindrical shell, respectively. The 3rd s-mode corresponds to the vibration modes (2,0), (4,0), (6,0), (8,0), and (10,0). The 5th s-mode corresponds to the vibration modes (2,1), (4,1), (6,1), (8,1), and (10,1). The 6th s-mode corresponds to the vibration modes (1,2), (3,2), (5,2), (7,2), and (9,2) of the cylindrical shell. Comparing Figures 3(a) and 3(b), it can be seen that the order of the s-modes changes except the 1st and 4th s-modes. In Figure 3(b), the 2nd s-modes have peaks at the vibration modes (2,0), (4,0), (6,0), (8,0), and (10,0). The 3rd s-mode corresponds to the vibration modes (1,1), (3,1), (5,1), (7,1), and (9,1). The 5th s-mode corresponds to the vibration modes (1,2), (3,2), (5,2), (7,2), and (9,2). The 6th s-mode corresponds to the vibration modes (2,1), (4,1), (6,1), (8,1), and (10,1) of the cylindrical shell. Therefore, it indicates that the shapes of the s-modes can help to determine the coupling relationship between the structure-dependent radiation modes and the vibration modes at low frequencies.

Figure 4 compares the contributions of the radiation modes to the radiated sound power at low frequencies. According to the literature [32], the 1st radiation modes (either s-mode or a-mode) contribute to over 95% of the total power for the beam and plate structure in the low-frequency range. For the cylindrical shell examined in this work, the contribution of the 1st radiation mode to the radiated sound power of the cylindrical shell is the only dominant radiation mode below 80 Hz, and it is no longer the dominant radiation mode above 80 Hz. The 1st radiation mode corresponds to the vibration modes with the circumferential modal index ($n = 0$), which has relatively higher natural frequency than those of the $n > 0$ circumferential modes. Different from reference [15], it is impossible to achieve radiated sound power attenuation in the low-frequency range by only controlling the first radiation mode. The sound power from the first four a-modes only coincided at some natural frequencies, and there are large differences at other frequency values. The sound power from first eight a-modes has a greater contribution to the radiated sound power, and at some natural frequencies such as 393, 735, and 948 Hz, the difference is significant. As the number of radiation modes increases, the contribution to the sound power increases. The sound power from first twelve a-modes could approximately represent the total radiated sound power, while for s-modes, only the first ten s-modes are needed. For active control, fewer modes can be controlled to achieve a better control effect, and at the same time, fewer sensors are needed to detect these modes, thus simplifying the control system construction.

3.2. Active Control. Based on the theory described above, the sound power radiating from a submerged cylindrical shell before and after applying control by secondary force input is investigated through a numerical simulation in this section. The geometry and material parameters of the cylindrical shell are given in Section 3.1. The primary excitation forces and secondary control forces are both harmonic point forces

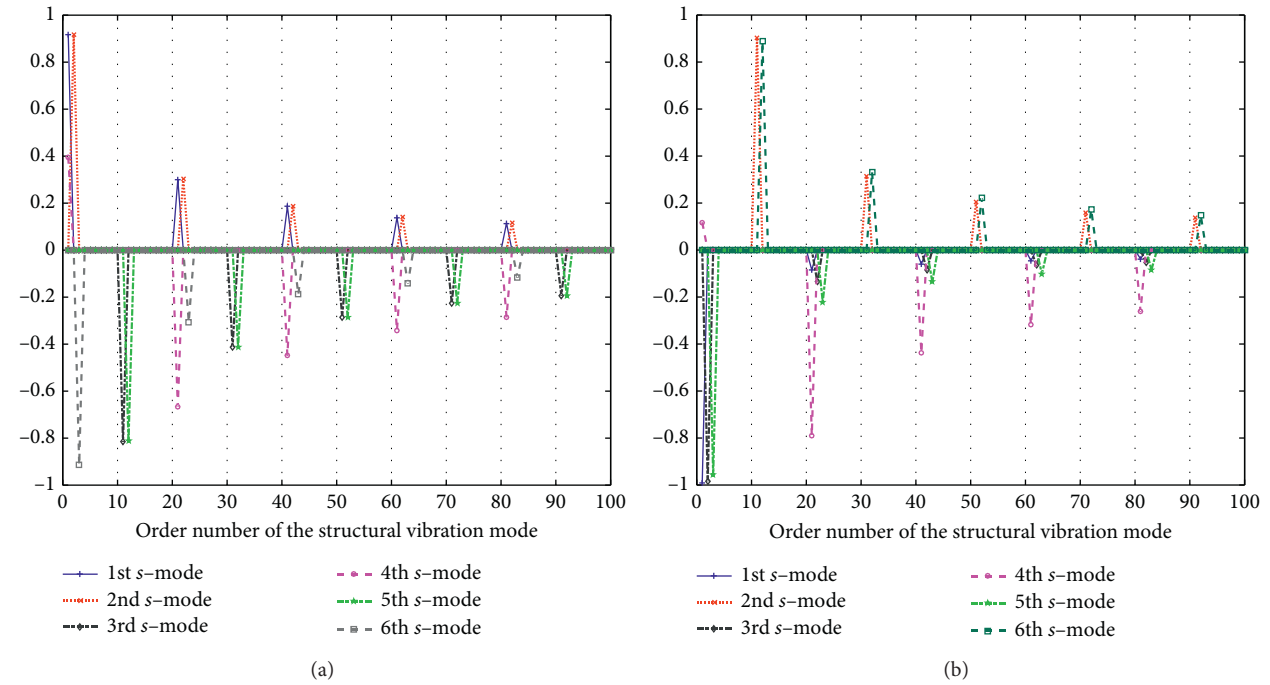

FIGURE 3: Modal shapes of the first six s-modes. (a) $kL = 1$; (b) $kL = 5$.

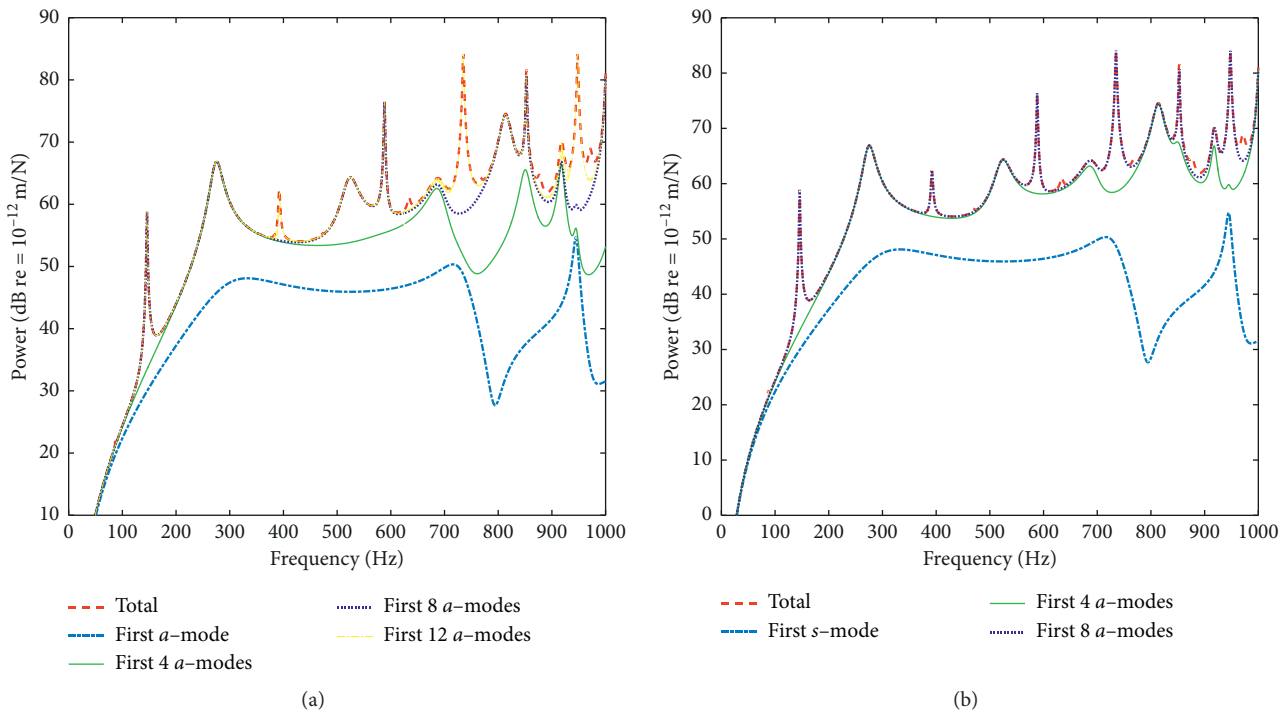

FIGURE 4: Radiated sound power from the first several a-modes and s-modes. (a) a-modes; (b) s-modes.

that are perpendicular to the surface of the shell. The position of the single primary excitation force is centered at a point $z_0 = 0.44$ and $\phi_0 = 0$, and its amplitude is 1 N. When two primary forces are used to excite the shell, the positions of the primary excitation forces are centered at a point $z_{01} = 0.44$ and $\phi_{01} = 0$ and $z_{02} = 0.3$ and $\phi_{02} = 0$, respectively, and the amplitudes are all 1 N. The minimization of the total sound power radiating from the cylindrical shell under primary excitation forces and secondary control forces is set as the target function. The amplitude and phase of the optimal control force are calculated using equation (28). The radiated sound power of the submerged finite cylindrical

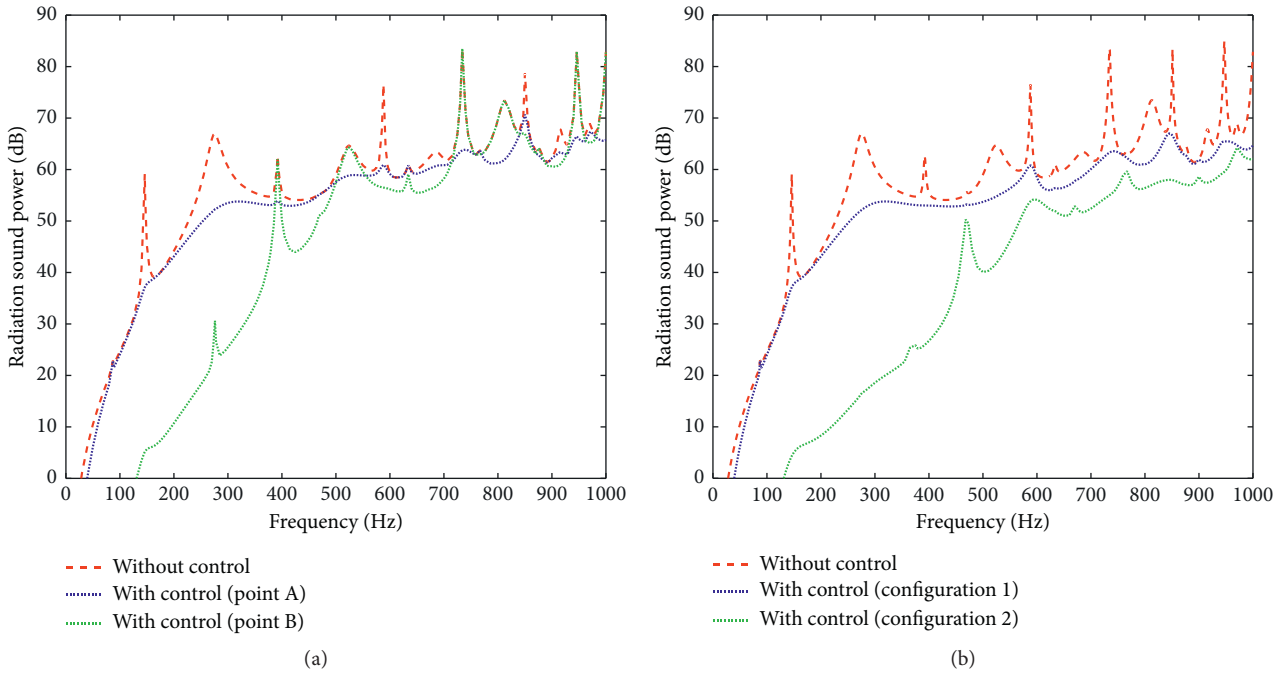

Figure 5: Effects of different positions and configurations of control force. (a) Single secondary control force. (b) Two secondary control forces.

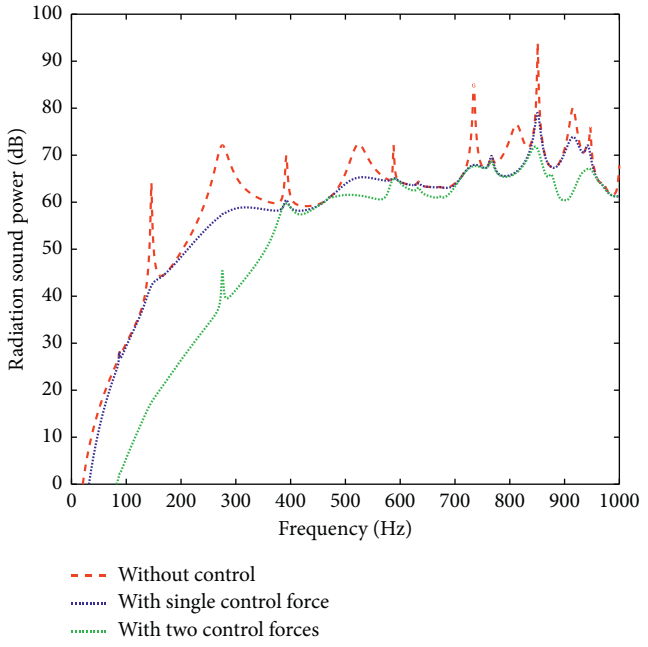

Figure 6: Comparison of control effects under multiple primary excitation forces.

shell before and after active control can be solved. Here, one and two secondary control forces are used for active control. First, when one force is used as a control force, the control effects of the secondary forces at different positions are compared. The effects of the two secondary control forces are also investigated. Figure 5 shows effects of different positions and configurations of control force under the single primary excitation force. Figure 5(a) shows the sound power radiating from the cylindrical shell before and after active control by different positions of the control forces located at point A (0.76, 180°) and B (0.6, 0°). Figure 5(b) shows the radiated sound power before and after active control by different configurations of the two control forces. One configuration consisted of two control forces located at

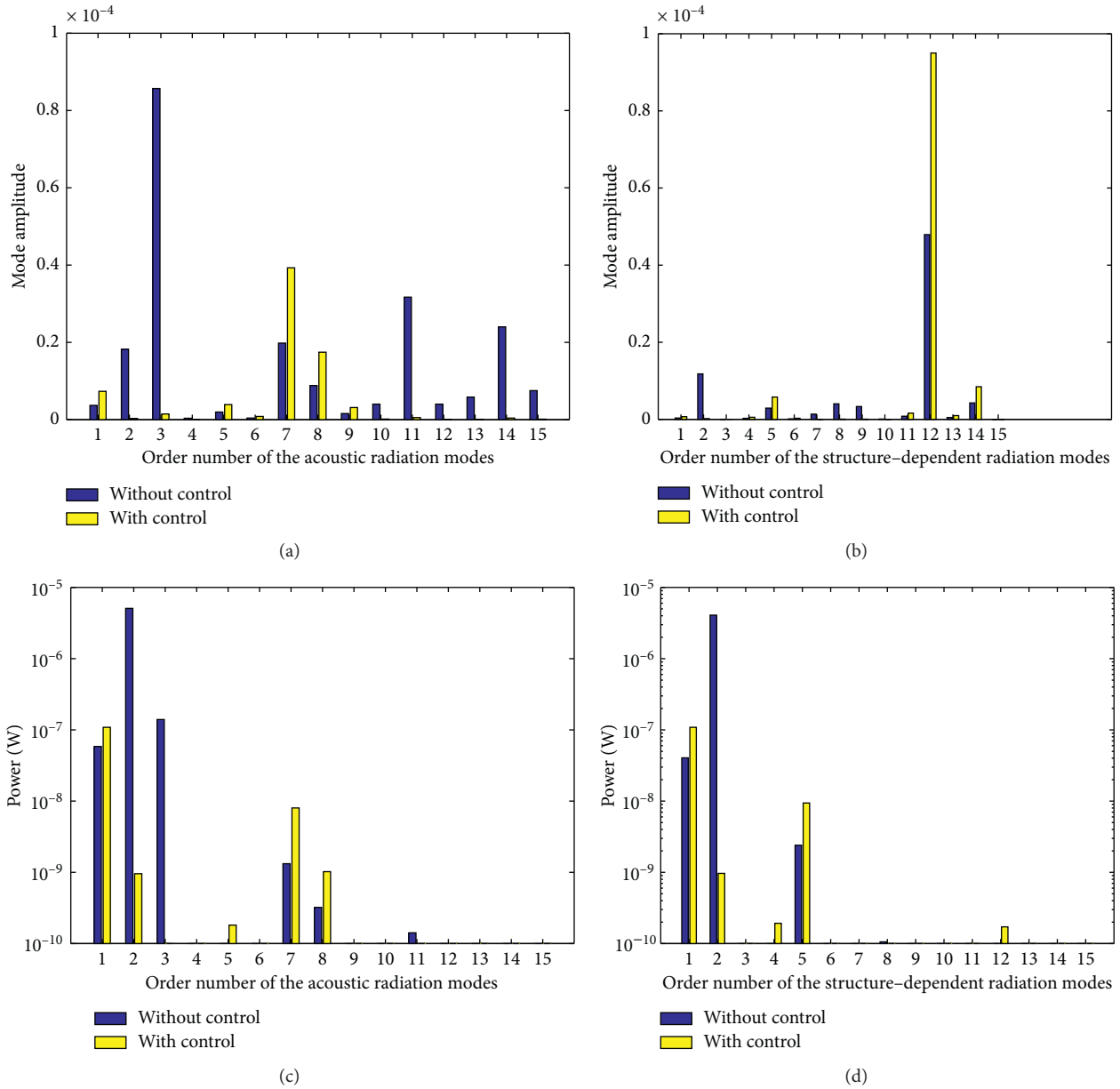

Figure 7: Amplitude and sound power of the *a*-modes and *s*-modes at resonance frequency (276 Hz). (a) Amplitude of the *a*-modes. (b) Amplitude of the *s*-modes. (c) Sound power of the *a*-modes. (d) Sound power of the *s*-modes.

point A (0.76, 180°) and C (0.44, 180°), and the other consisted of two control forces located at point A (0.76, 180°) and D (0.6, 0°). Figure 6 compared the control effects of two control forces under multiple primary excitation forces, and the single control force is located at point A (0.76, 180°), and the two control forces are located at point A (0.76, 180°) and C (0.9, 0°).

When a single primary force is used to excite the shell and a single secondary control force located at point A is used for active control, the peaks of the radiated sound power at most resonance frequencies have significant attenuation, as shown in Figure 5(a). With the single secondary control force located at point B, the larger attenuation appears in the low-frequency range. In the range from 380 to 1000 Hz, the control effect is unsatisfactory at resonance frequencies and not as good as that with the secondary force located at point A. The main reason for this is that the secondary force located at point A is at the antinodal line relative to primary excitation forces, but the secondary force located at point B is at the nodal line of the even-order axial vibration modes. Therefore, the optimal control effect may be achieved by searching for the optimal position of the secondary control force. Comparing the results shown in Figures 5(a) and 5(b), it is evident that the radiated sound power in the frequency range of interest is reduced significantly by the two control forces, and the control effect is superior to single control force. In addition, the position of the two secondary control forces also has a

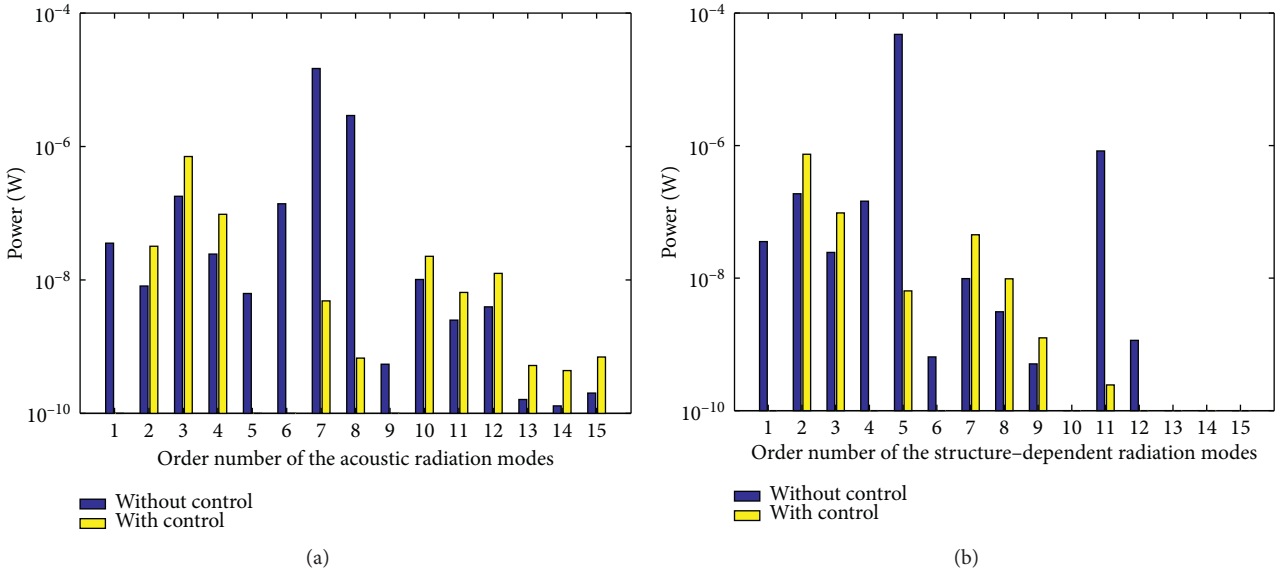

FIGURE 8: Sound power of the *a*-modes and *s*-modes at resonance frequency (588 Hz). (a) Sound power of the *a*-modes. (b) Sound power of the *s*-modes.

significant influence on the control effect. It can be seen from Figure 6 that there also have good control effects at most resonant frequencies for single control force when two primary forces are used to excite the shell. The results suggest that the control effect can be improved by increasing the number of control forces for the entire frequency band. The results show that the sound power radiated from the submerged vibrating cylindrical shell could be attenuated by suppressing the vibrating parts of the shell through the vibrators placed on the shell used to generate the secondary control force. For the shell subjected to a complex excitation, the structural acoustic radiation may be controlled by placing multiple exciters and optimizing the position, input amplitude, and phase of the vibration exciters.

3.3. Physical Mechanism of Active Control. To understand the influence of the modal amplitude on the sound power radiated from the cylindrical shell before and after active control, the control mechanisms are analyzed from the perspective of the radiation modes. In this section, the primary excitation force is the same as that in the previous section, and a single radial force is used as a secondary control force located at position A on the cylindrical shell. Modal amplitude changes at the resonance frequencies of 276 Hz (1,1) and 588 Hz (3,2) and the nonresonance frequency of 500 Hz are considered as examples. The amplitude and sound power of the *a*-modes and *s*-modes at these frequencies are shown in Figures 7–9. The blue bars of the column plot represent the modal amplitude and sound power before control, and the yellow bars represent those after control.

As shown in Figures 7(a) and 7(b), there is only one dominant peak of the first 15 *a*-modes and *s*-modes at the resonance frequency of 276 Hz before control, the 2nd *a*-mode and the 12th *s*-mode. After applying the control, the amplitude of the 2nd *a*-mode decreases sharply, while the amplitude of the 12th *s*-mode increases. This indicates that the 12th *s*-mode is not the dominant mode. According to equations (12) and (20), the contribution of the *a*-mode or *s*-mode on the sound radiation power is determined by the multiplication of the radiation coefficient and amplitude of the radiation mode. Consequently, we must calculate the radiated sound power for each *a*-mode and *s*-mode. Figures 7(c) and 7(d) show the radiated sound power of the first 15 *a*-modes and *s*-modes before and after applying control. For the *a*-modes, the maximum peaks of the sound power as well as amplitude of the radiation mode occur for the second-order mode. Different from the amplitude of the *s*-modes, the maximum peak of the sound power of the *s*-modes occurs for the second-order mode and decreases significantly after control is applied, which shows the 2nd *s*-mode is the dominant mode at 276 Hz. In the subsequent analysis, the radiated sound power for each *a*-mode and *s*-mode before and after control is used to display the control mechanism.

Figures 8(a) and 8(b) show the amplitude and power of the *a*-modes and *s*-modes at the resonance frequency of 588 Hz. In Figure 8(a), the 7th and 8th *a*-modes have higher amplitudes, and these two modes are pairs of acoustic radiation modes with the same modal shape but a 90° phase shift, as shown in Figure 2. After applying control, the sound power in the 7th and 8th *a*-modes decreases. As shown in Figure 8(b), the 5th *s*-mode is the dominant structure-dependent radiation mode, and the amplitude that attenuates significantly after control is applied.

Furthermore, Figures 9(a) and 9(b) show that the sound power radiated from some *s*-modes or *a*-modes decrease after applying control at nonresonance frequency. When some radiation modal sound power increase, the sum of the sound power from all the radiation modes remains almost unchanged before and after control. This occurs mainly because there is no dominant structural vibration mode at the nonresonance frequency and no dominant radiation

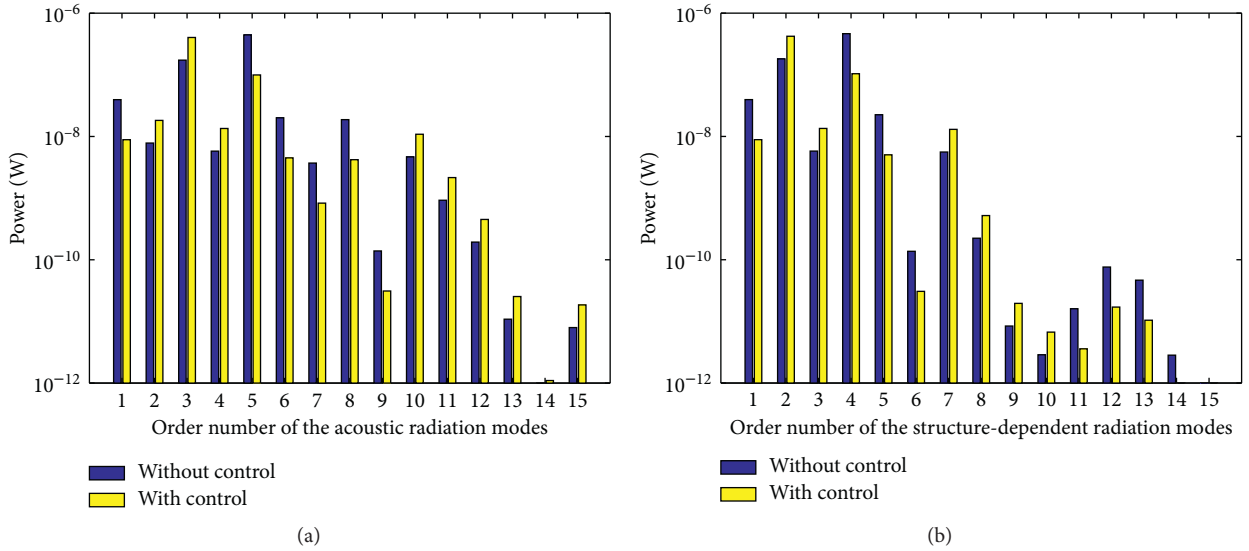

FIGURE 9: Sound power of the *a*-modes and *s*-modes at nonresonance frequency (500 Hz). (a) Sound power of the *a*-modes. (b) Sound power of the *s*-modes.

mode. In particular, Figure 9(a) shows that the 3rd and 5th *a*-modes contribute more to the radiated sound power than the other modes. After applying control, the radiated sound power for the 3rd *a*-mode increases, while that of the 5th *a*-mode decreases. The *s*-modes are slightly different from the *a*-modes. As shown in Figure 9(b), the peaks of the radiated sound power correspond to the 2nd and 4th *s*-modes. The sound power radiation of the 2nd *s*-mode increases, while that of the 5th *a*-mode decreases after control is applied.

Therefore, when the minimum of the total sound power radiating from a cylindrical shell is considered as the control target, the mechanism of active control is used to reduce the sound power of the dominant *a*-modes or *s*-modes corresponding to structural vibration modes, while ensuring that the magnitude of the nondominant radiation modes is not significantly increased, allowing the sound radiation of the vibrating structure to be controlled.

4. Conclusion

The radiation characteristics and active structural acoustic control of a submerged cylindrical shell at low frequencies are investigated by means of the radiation modes. The contribution of the low-order radiation modes to the radiated sound power is discussed. The results show that the sound power radiated from a group of specific vibration modes can be replaced by that generated through one *a*-mode or *s*-mode. The performance of the sound power radiated from individual radiation modes decreases with the increase in the mode number. Only the first few radiation modes contribute to the sound power radiated from a submerged finite cylindrical shell at low frequencies. However, the contribution of the first radiation mode of the cylindrical shell to the radiated sound power at the low frequency is not always dominant mode, especially at higher resonant frequencies.

The active structural acoustic control of a submerged finite cylindrical shell is investigated by considering the fluid-structure coupled interaction. The analytical expression of the optimal complex amplitude of the secondary force is derived based on the uncoupled characteristics of the radiated sound power in the circumferential direction, and the control effects with one and two control forces are also compared. Moreover, the physical mechanism of the active structural acoustic control of the submerged finite cylindrical shell is analyzed based on the radiation modes. The results show that a greater reduction is achieved using multiple secondary forces by controlling the vibration of the shell, which effectively produces the sound radiation. The physical mechanism of the active control is to reduce the amplitude of the radiation modes corresponding to the structural vibration modes, thereby effectively controlling the sound radiated due to structural vibrations.

Appendix

A. Flügge Operator

The elements of the Flügge operator $\mathbf{L}_{3\times3}$ in equation (1) are given as

$$L_{11} = a^2\frac{\partial^2}{\partial z^2} + \left(\frac{1-\sigma}{2}\right)(1+\beta)\frac{\partial^2}{\partial \phi^2} - \frac{\rho_s a^2\left(1-\sigma^2\right)}{E^*}\frac{\partial^2}{\partial t^2},$$

$$L_{12} = L_{21} = a\frac{1+\sigma}{2}\frac{\partial^2}{\partial z \partial \phi},$$

$$L_{13} = L_{31} = \sigma a\frac{\partial}{\partial z} + \beta a\frac{(1-\sigma)}{2}\frac{\partial^3}{\partial z\,\partial \phi^2} - ka^3\frac{\partial^3}{\partial z^3},$$

$$L_{22} = a^2\frac{1-\sigma}{2}(3\beta+1)\frac{\partial^2}{\partial z^2} + \frac{\partial^2}{\partial \phi^2} - \frac{\rho a^2\left(1-\sigma^2\right)}{E^*}\frac{\partial^2}{\partial t^2},$$

$$L_{23} = L_{32} = \frac{E^* h}{a^2\left(1-\sigma^2\right)}\left(\frac{\partial}{\partial \phi} - \beta a^2\frac{(3-\sigma)}{2}\frac{\partial^3}{\partial \phi\,\partial z^2}\right),$$

$$L_{33} = 1 + \beta + 2\beta\frac{\partial^2}{\partial \phi^2} + \beta\nabla^4 - \frac{\rho a^2\left(1-\sigma^2\right)}{\tilde{E}}\frac{\partial^2}{\partial t^2},$$

(A.1)

where $\nabla^4 = a^4(\partial^4/\partial z^4) + 2a^2(\partial^4/\partial z^2\partial\phi^2) + (\partial^4/\partial\phi^4)$, $\beta = h^2/12a^2$, and ρ_s denotes the density of the cylindercal shell.

B. The Expression for Modal Sound Pressure

It is assumed that a finite-length cylindrical shell with simple supports at both ends is immersed in an irrotational, nonviscous, and compressible fluid. The vibration of the shell causes the vibration of the surface medium, and the sound field is generated. For the steady-state problem, the pressure field satisfies the acoustic wave equation in cylindrical coordinates:

$$\nabla^2 p_a + k^2 p_a = 0, \tag{B.1}$$

where ∇^2 is the Laplace operator in cylindrical coordinates.

According to the continuity condition, the radial velocity of the fluid is equal to the radial vibration velocity of the structure on the contact surface between the fluid and the structure, and no cavitation is assumed at the fluid-shell interface at $r = a$:

$$\frac{\partial p_a}{\partial r}|_{r=a} = \rho_l \omega^2 C^{\alpha}_{wnm}. \tag{B.2}$$

The Sommerfeld radiation condition is satisfied at an infinite distance:

$$\lim_{r\longrightarrow\infty} r\left(\frac{\partial p_a}{\partial r} + ikp_a\right) = 0. \tag{B.3}$$

The Green's function satisfies the Neumann boundary condition for a finite-length cylindrical shell with an infinite barrier. Thus, the radiated sound pressure of the cylindrical shell is expressed as

$$p_a(\mathbf{r}) = -i\rho_l\omega\iint G\left(\frac{\mathbf{r}}{\mathbf{r}_0}\right)\dot{w}(\mathbf{r}_0)dS, \tag{B.4}$$

where $\mathbf{r}$ denotes the points on the outside of the cylindrical shell and $\mathbf{r}_0$ denotes the points on the cylindrical shell.

In cylindrical coordinates, Green's function satisfying the above equation can be expressed as

$$G\left(\frac{\mathbf{r}}{\mathbf{r}_0}\right) = -\frac{1}{4\pi^2}\sum_{n=0}^{\infty}\varepsilon_n\cos\left[n(\phi-\phi_0)\right]\cdot\int_{-\infty}^{\infty}\frac{H_n^{(1)}\left(\sqrt{k^2-k_z^2}\,r\right)}{\sqrt{k^2-k_z^2}\,aH_n^{(1)\prime}\left(\sqrt{k^2-k_z^2}\,a\right)}e^{jk_z(z-z_0)}dk_z. \tag{B.5}$$

By substituting $w(z,\phi)$ in equations (2) and (B.5) into equation (B.4), the radiated sound pressure of a cylindrical shell of finite length simply supported at both ends can be obtained:

$$p_a(\mathbf{r}) = \frac{\omega^2\rho_l}{2\pi}\sum_{\alpha=0}^{1}\sum_{n=0}^{\infty}\sum_{m=1}^{\infty}C^{\alpha}_{wnm}\sin\left(n\phi+\frac{\alpha\pi}{2}\right)\int_{-\infty}^{\infty}\tilde{Z}(k_z)\psi_m(k_z)e^{ik_z z}dk_z, \tag{B.6}$$

where

$$\psi_m(k_z) = \int_0^L \sin\left(\frac{m\pi z}{L}\right)e^{-ik_z z}dz. \tag{B.7}$$

At the surface of the cylindrical shell, the surface sound pressure of the shell can be expanded according to the mode function of the cylindrical shell:

$$p_a = \sum_{\alpha=0}^{1}\sum_{m=1}^{\infty}\sum_{n=1}^{\infty}P^{\alpha}_{mn}\sin\left(n\phi_0+\frac{\alpha\pi}{2}\right)\sin(k_m z_0). \tag{B.8}$$

According to the radiated sound pressure of the cylindrical shell, the surface modal sound pressure can be expressed by using the orthogonality of trigonometric functions as

$$P^{\alpha}_{mn} = -i\omega a\sum_{q=1}^{\infty}C^{\alpha}_{wmn}Z_{qmn}, \tag{B.9}$$

where Z_{qmn} is the radiation impedance, which expresses the modal coupling between the different axial modal indices (m and q) due to the fluids.

Data Availability

The data used to support the findings of this study are included within this article.

Conflicts of Interest

The authors declare that they have no conflicts of interest.

Acknowledgments

This research was supported by the National Natural Science Foundation of China (Grant nos. 11764002 and 51765001) and the Key Scientific Research Project of North Minzu University (Grant no. 2019KJ34). The authors thank LetPub (http://www.letpub.com) for its linguistic assistance and scientific consultation during the preparation of this paper.

References

[1] B. Laulagnet and J. L. Guyader, "Sound radiation by finite cylindrical ring stiffened shells," *Journal of Sound and Vibration*, vol. 138, no. 2, pp. 173–191, 1990.

[2] P. R. Sepanishen, "Radiated power and radiation loading of cylindrical surfaces with non-uniform velocity distributions," *Journal of the Acoustical Society of America*, vol. 63, no. 2, pp. 328–338, 1978.

[3] B. Laulagnet and J. L. Guyader, "Modal analysis of a shell's acoustic radiation in light and heavy fluids," *Journal of Sound and Vibration*, vol. 131, no. 3, pp. 397–415, 1989.

[4] F. Bérot and B. Peseux, "Vibro-acoustic behavior of submerged cylindrical shells: analytical formulation and numerical model," *Journal of Fluids and Structures*, vol. 12, no. 8, pp. 959–1003, 1998.

[5] M. Caresta and N. J. Kessissoglou, "Structural and acoustic responses of a fluid-loaded cylindrical hull with structural discontinuities," *Applied Acoustics*, vol. 70, no. 7, pp. 954–963, 2009.

[6] M. C. Junger, "Radiation loading of cylindrical and spherical surfaces," *The Journal of the Acoustical Society of America*, vol. 24, no. 3, pp. 288-289, 1952.

[7] B. E. Sandman, "Fluid-loading influence coefficients for a finite cylindrical shell," *The Journal of the Acoustical Society of America*, vol. 60, no. 6, pp. 1256–1264, 1976.

[8] M. Amabili, "Flexural vibration of cylindrical shells partially coupled with external and internal fluids," *Journal of Vibration and Acoustics*, vol. 119, no. 3, pp. 476–484, 1997.

[9] M. Amabili, "Vibrations of circular tubes and shells filled and partially immersed in dense fluids," *Journal of Sound and Vibration*, vol. 221, no. 4, pp. 567–585, 1999.

[10] M. Amabili, *Nonlinear Vibrations and Stability of Shells and Plates*, Cambridge University Press, New York, NY, USA, 2008.

[11] M. K. Kwak, "Free vibration analysis of a finite circular cylindrical shell in contact with unbounded external fluid," *Journal of Fluids and Structures*, vol. 26, no. 3, pp. 377–392, 2010.

[12] K. Naghshineh, W. Chen, and G. H. Koopmann, "Use of acoustic basis functions for active control of sound power radiated from a cylindrical shell," *The Journal of the Acoustical Society of America*, vol. 103, no. 4, pp. 1897–1903, 1998.

[13] J. P. Maillard and C. R. Fuller, "Active control of sound radiation from cylinders with piezoelectric actuators and structural acoustic sensing," *Journal of Sound and Vibration*, vol. 222, no. 3, pp. 363–387, 1999.

[14] X. Pan, Y. Tso, and R. Juniper, "Active control of low-frequency hull–radiated noise," *Journal of Sound and Vibration*, vol. 313, no. 2, pp. 29–45, 2008.

[15] A. Loghmani, M. Danesh, M. K. Kwak, and M. Keshmiri, "Active control of radiated sound power of a smart cylindrical shell based on radiation modes," *Applied Acoustics*, vol. 114, no. 1, pp. 218–229, 2016.

[16] M. Caresta and N. J. Kessissoglou, "Active control of sound radiated by a submarine hull in axisymmetric vibration using inertial actuators," *Journal of Vibration and Acoustics*, vol. 81, pp. 1–8, 2012.

[17] Y. Cao, H. Sun, F. Y. An, and X. Li, "Active control of low-frequency sound radiation by cylindrical shell with piezoelectric stack force actuators," *Journal of Sound and Vibration*, vol. 331, no. 11, pp. 2471–2484, 2012.

[18] M. X. Chen, D. P. Luo, G. Cao, F. Zhou, and H. L. Guo, "Sound radiation analysis of low order modes from finite stiffened double cylindrical shells," *Journal of Harbin Engineering University*, vol. 25, no. 4, pp. 446–450, 2004.

[19] T. R. Lin, M. Chris, and O. S. Peter, "Characteristics of modal sound radiation of finite cylindrical shells," *Journal of Vibration and Acoustics*, vol. 133, no. 5, pp. 1–6, 2011.

[20] H. Peters, N. J. Kessissoglou, and S. Marburg, "Modal decomposition of exterior acoustic-structure interaction," *Journal of the Acoustical Society of America*, vol. 133, no. 5, pp. 2668–2677, 2013.

[21] O. M. Fein, L. Gaul, and U. Stobener, "Vibration reduction of a fluid-loaded plate by modal control," *Journal of Intelligent Material Systems and Structures*, vol. 16, no. 6, pp. 541–552, 2005.

[22] S. Li, "Active modal control simulation of vibro-acoustic response of a fluid-loaded plate," *Journal of Sound and Vibration*, vol. 330, no. 23, pp. 5545–5557, 2011.

[23] S. J. Elliott and M. E. Johnson, "Radiation modes and the active control of sound power," *Journal of the Acoustical Society of America*, vol. 94, no. 4, pp. 2194–2204, 1993.

[24] K. A. Cunefare, "Effect of modal interaction on sound radiation from vibrating structures," *AIAA Journal*, vol. 30, no. 12, pp. 2819–2828, 1992.

[25] K. A. Cunefare and M. N. Currey, "On the exterior acoustic radiation modes of structures," *Journal of the Acoustical Society of America*, vol. 96, no. 4, pp. 2302–2312, 1994.

[26] K. A. Cunefare, M. N. Currey, M. E. Jonhnson, and S. J. Elliott, "The radiation efficiency grouping of free-space acoustic radiation modes," *Journal of the Acoustical Society of America*, vol. 109, no. 1, pp. 203–215, 2001.

[27] K. Naghshineh and G. H. Koopmann, "Active control of sound power using acoustic basis functions as surface velocity filters," *Journal of the Acoustical Society of America*, vol. 93, no. 5, pp. 2740–2752, 1993.

[28] W. R. Johnson, P. Aslani, and D. R. Hendricks, "Acoustic radiation mode shapes for control of plates and shells," *Journal of the Acoustical Society of America*, vol. 133, no. 5, pp. 3385-3386, 2013.

[29] D. R. Wilkes, H. Peters, P. Croaker, S. Marburg, A. J. Duncan, and N. Kessissoglou, "Non-negative intensity for coupled fluid–structure interaction problems using the fast multipole

method," *Journal of the Acoustical Society of America*, vol. 141, no. 6, pp. 4278–4288, 2017.

[30] S. H. Ding, K. A. Chen, and X. Y. Ma, "Analysis of low frequency radiation characteristics of a finite cylindrical shell based on vibration and radiation modes," in *Proceedings of the 21st International Congress on Sound and Vibration*, pp. 13–17, Beijing, China, July, 2014.

[31] D. M. Photiadis, "The relationship of singular value decomposition to wave-vector filtering in sound radiation problems," *Journal of the Acoustical Society of America*, vol. 88, no. 2, pp. 1152–1159, 1990.

[32] L. Ji and J. S. Bolton, "Sound power radiation from a vibrating structure in terms of structure-dependent radiation modes," *Journal of Sound and Vibration*, vol. 335, pp. 245–260, 2015.

[33] X. Pan, Y. Tso, and R. Juniper, "Active control of radiated pressure of a submarine hull," *Journal of Sound and Vibration*, vol. 311, no. 1-2, pp. 224–242, 2008.

[34] M. Caresta and N. J. Kessissoglou, "Active control of sound radiated by a submarine in bending vibration," *Journal of Sound and Vibration*, vol. 330, no. 4, pp. 615–624, 2011.

[35] X. L. Ma, G. Y. Jin, and Z. G. Liu, "Active structural acoustic control of an elastic cylindrical shell coupled to a two-stage vibration isolation system," *International Journal of Mechanical Sciences*, vol. 79, pp. 182–194, 2014.

[36] S. Merz, N. J. Kessissoglou, R. Kinns, and S. Marburg, "Passive and active control of the radiated sound power from a submarine excited by propeller forces *Journal of Ship Research*, vol. 57, no. 1, pp. 59–71, 2013.

[37] S. X. Liu and M. S. Zou, "Evaluation of radiation loading on finite cylindrical shells using the fast Fourier transform: a comparison with direct numerical integration," *Journal of the Acoustical Society of America*, vol. 143, no. 3, pp. 160–166, 2018.

[38] Y. Sun, T. J. Yang, and Y. H. Chen, "Sound radiation modes of cylindrical surfaces and their application to vibro-acoustics analysis of cylindrical shells," *Journal of Sound and Vibration*, vol. 424, pp. 64–77, 2018.

[39] P. Liu, "The impact of diving depth on vibration and acoustic radiation of cylinderical shell and research of similarity," Master's Thesis, Dalian University of Technology, Dalian, China, 2013.

[40] A. Ergin, W. G. Price, R. Randall, and P. Temarel, "Dynamic characteristics of a submerged, flexible cylinder vibrating in finite water depths," *Journal of Ship Research*, vol. 36, no. 2, pp. 154–167, 1992.